Journal of Nuclear Materials 393 (2009) 12–21

Contents lists available at ScienceDirect

Journal of Nuclear Materials

journal homepage: www.elsevier.com/locate/jnucmat

The change in the hardness of LCAC, TZM, and ODS molybdenum in the post-irradiated and annealed conditions

B.V. Cockeram [a,*], R.W. Smith [a], T.S. Byun [b], L.L. Snead [b]

[a] Bechtel-Bettis Inc., P.O. Box 79, West Mifflin, PA 15122-0079, USA
[b] Oak Ridge National Laboratory, P.O. Box 2008, Oak Ridge, TN 37831-6138, USA

ARTICLE INFO

Article history:
Received 10 December 2008
Accepted 27 April 2009

ABSTRACT

Hardness measurements were performed on wrought Low Carbon Arc Cast (LCAC), TZM, and Oxide Dispersion Strengthened (ODS) molybdenum in the post-irradiated and post-irradiated + annealed condition to determine the recovery kinetics. Irradiations performed in the High Flux Isotope Reactor (HFIR) at nominally 300 °C and 600 °C to neutron fluence levels that range from 10.5 to 246×10^{24} n/m^2 ($E > 0.1$ MeV) resulted in relatively large increases in hardness (77–109%), while small increases in hardness (<18%) were observed for irradiations at 870–1100 °C. The hardness recovery for ODS and LCAC irradiated at 300 °C and 600 °C were shown to be complete at 980 °C and ≈ 1100–1250 °C, respectively. Isothermal annealing at 700 °C was used to determine the activation energy for recovery of LCAC and ODS (3.70–4.88 eV ± 0.28–0.77 eV), which is comparable to values reported in the literature for molybdenum vacancy self-diffusion. This suggests that recovery of LCAC and ODS is controlled by the solid-state diffusion of vacancies in the bulk, and that the finer grain size and particle size ODS does not affect this mechanism. TZM exhibited slower recovery kinetics, which can be explained by the solute atoms (titanium and zirconium) inhibiting vacancy diffusion.

1. Introduction

Molybdenum has a relatively high melting point of 2610 °C, excellent strength and creep-resistance at high temperatures, and typically possesses measurable ductility at room-temperature when the grain boundary impurities are controlled [1–7]. These properties have lead to an interest in the use of molybdenum for vacuum furnace components, forging dies, and advanced energy applications. Irradiation of molybdenum at temperatures of 600 °C or less generally results in the formation of a high number density of voids and/or loops that restrict dislocation motion and produce hardening [2–26]. Irradiation hardening can result in embrittlement for some molybdenum alloys by elevation of the flow stress above the fracture stress. This leads to an increase in the Ductile to Brittle Transition Temperature (DBTT). Wrought molybdenum alloys with fine, elongated grains, such as ODS molybdenum [24,26] or high-purity molybdenum [21,26], have exhibited resistance to irradiation embrittlement. A room-temperature DBTT was observed for 600 °C irradiated ODS that is lower than the DBTT of 300 °C and 700 °C observed for LCAC and TZM, respectively, irradiated under the same conditions [23,24]. Irradiation of the materials at 300 °C, however, produces a much finer spacing of voids and loops and their embrittling effect overwhelms the various differences in materials microstructure. For these irradiations, the same DBTT of 800 °C was observed for ODS, LCAC, and TZM [23,24]. High purity molybdenum and ODS molybdenum in the as-worked condition have exhibited lower DBTT values of 450 °C and −50 °C for irradiations at 300 °C and 600 °C, respectively, to much lower fluences (1.29–0.01 dpa-Mo) than obtained in this work [26]. This indicates higher purity and increased dislocation density can provide improved resistance to irradiation embrittlement and less hardening for low fluence irradiations [26]. Irradiation at temperatures of 800 °C or higher, where the point defects have greater mobility, generally produces a lower number density of coarse voids that result in substantially less hardening and little embrittlement in any of the molybdenum materials studied [23,24].

Post-irradiation hardness measurements provide a method for quantifying irradiation hardening and providing an indirect measure of the density of defects that restrict dislocation motion. Many authors have studied the change in defect density during post-irradiated annealing using hardness and electrical resistivity measurements [3,6–13,18,25–44]. These studies have mainly used electrical resistivity methods while the studies that have utilized hardness measurements are generally conducted at a single irradiation temperature and single neutron fluence. Only recently was the Meechan–Brinkman analysis of isochronal and isothermal annealing results [45–47] used to determine the activation energy for post-irradiation recovery for unalloyed Low Carbon Arc Cast (LCAC) molybdenum. It was shown to be comparable to values for molybdenum vacancy self-diffusion for irradiations at 270 °C

* Corresponding author. Tel.: +1 412 476 5647; fax: +1 412 476 5779.
E-mail address: cockeram@bettis.gov (B.V. Cockeram).

0022-3115/$ - see front matter © 2009 Elsevier B.V. All rights reserved.
doi:10.1016/j.jnucmat.2009.04.025

Table 1
Certification chemistries, grain sizes, and DBTT for the LCAC sheet, ODS sheet, and TZM plate (in weight ppm) [22–25].

Material/lot#	C	O	N	Ti	Zr	Fe	Ni	Si	La	Al	Ca	Cr	Cu	Other
LCAC sheet Ingot 40386A2sheet Heat# C18605 0.51 mm sheet	90	3	4	NA	NA	10	<10	<10	NA	NA	NA	NA	NA	NA
LCAC specification[1]	⩽100	⩽15	⩽20	NA	NA	⩽100	⩽20	⩽100	NA	NA	NA	NA	NA	NA
TZM plate Ingot 61722B Heat# TZM24080 6.35 mm plate	223	17	9	5000	1140	<10	<10	<10	NA	NA	NA	NA	NA	NA
TZM Specification[1]	100/300	⩽30	⩽20	4000/5500	600/1200	⩽100	⩽20	⩽100	NA	NA	NA	NA	NA	NA
ODS Sheet ODS Mo ingot 32438 Heat# LA 23795 0.76 mm sheet	40	NA	NA	<10	NA	27	<10	<10	1.08 wt%	<10	<10	<10	<10	<10 Mg <10 Pb <10 Sn

Grain Size	Grain width (μm)		Grain length (μm)		Pre-irradiation DBTT (°C)	Post-irradiated DBTT for various nominal irradiation temperatures (°C)		
	Average	Standard deviation	Average	Standard deviation		300	600	900
LCAC sheet – LSR	3.9	2.5	172	79.0	−100	800	300	−50
LCAC sheet – TSR	5.0	2.7	78.1	38.2	−100	N/A	N/A	<25
TZM plate – LSR	3.9	2.5	273	105	−50	800	700	−50
TZM plate – TSR	6.1	3.8	132	69	−50	N/A	700	<0
ODS sheet – LSR	1.2	0.8	45.7	25.0	−100	800	25	−100
ODS sheet – TSR	2.5	1.0	33.3	12.1	25	N/A	>25	<300

[1]ASTM B386 – 365 for arc-cast LCAC and B386 – 363 for TZM [48].
[2]NA = Not available.
[3]All material was obtained from H.C. Stark, which was formally known as CSM Industries, Inc., Cleveland, OH.
[4]Trace GDMS composition for elements not listed was <1 ppm.
[5]All of these molybdenum alloys were wrought processed, and the grain structure consists of sheet-like, pancaked grains that are aligned in the longitudinal orientation.

and 605 °C to fluences between 10.5 and 27.0×10^{24} n/m^2 [25]. No previously published study of post-irradiation recovery kinetics in molybdenum has used a range of irradiation temperatures, neutron fluences, and different starting microstructures. The purpose of this work is to determine the change in hardness for three different wrought molybdenum alloys that have different grain sizes, compositions, and particle distributions as functions of neutron dose ($10.5–247 \times 10^{24}$ n/m^2) and irradiation temperature (270–1100 °C) following irradiation and post-irradiation annealing and to determine the kinetics for point defect mobility. The materials selected for study are LCAC, TZM, and ODS molybdenum, for which tensile results were previously reported [22–24]. TZM and LCAC have similar grain sizes (Table 1), but TZM contains carbon, titanium, and zirconium that form carbide precipitates with some titanium and zirconium in solid-solution resulting in improved high-temperature strength. Oxide Dispersion Strengthened (ODS) molybdenum contains 2vol.% La-oxide particles that stabilize a finer grain size and improve the high-temperature strength [49–53].

2. Materials and experimental procedure

The LCAC sheet (0.51 mm thick), ODS sheet (0.76 mm), and TZM plate (6.35 mm) were procured from H.C. Starck, Inc., see Table 1. These are the same heats used in previous work, and the processing has been described [21–25]. LCAC and TZM are produced by vacuum arc melting, hot extrusion, and hot rolling into sheet or plate, with a final Stress-Relief (SR) anneal at 850 °C/1 h for LCAC and 1150 °C/0.5 h for TZM. ODS was produced by wet doping Mo-oxide powder with a La-nitrate solution, conversion to molybdenum powder with fine La-oxide particles, consolidation into a billet, hot extrusion, hot rolling into sheet, and a SR anneal at 1200 °C/1 h [50–54]. Sub-sized SS-1 flat tensile specimens were machined in the longitudinal (LSR) or transverse (TSR) orientations, laser-scribed for identification, electropolished, and then SR annealed again at the appropriate temperature [22–25]. Discs (3 mm diameter × 0.25 mm thick) for Transmission Electron Microscopy (TEM) were machined in the through thickness orientation.

The irradiation of eight tensile specimens and eight TEM discs were performed at nominally 300 °C (270–384 °C), 600 °C (560–609 °C), and 900 °C (870–936 °C) to fluences between 10.5 and 247×10^{24} n/m^2 in the High Flux Isotope Reactor (HFIR) using conditions that have been described [22–25], see Table 2. All capsules were irradiated in the peripheral target tube position (PTP) of HFIR at 85 MW of power in the nominal neutron spectrum that is produced by HFIR, with a nominal peak fast neutron flux of 10×10^{18} n/m^2–sec ($E > 0.1$ MeV) and a peak thermal neutron flux of 2.2×10^{19} n/m^2–sec ($E < 0.5$ MeV). Passive SiC temperature monitors were use to determine the specimen temperatures. The transmutation products produced by irradiation of molybdenum in HFIR to the fluence values in Table 2 (3.3 and 10.6 dpa) are calculated to be very low in concentration (<0.2 and 0.6 wt%) and are primarily Tc and Ru with 3–4 ppm amounts of Zr and Nb [54,55]. Independent calculations of the transmutation products that would result from irradiation to these fluences using an ORIGEN-S point depletion computer program were previously shown [22–25] to be consistent with the concentrations of transmutation products that were reported by Greenwood and Garner [55]. The irradiation hardening observed for molybdenum alloys is believed to primarily be the result of the agglomeration of point defects to produce hardening barriers [22–25]. A saturation of the increase in tensile strength and irradiation hardening is observed at higher neutron fluences [22–25]. Since the amount of transmutation products are increased at higher neutron fluences, these results indicate that the defects resulting from irradiation have a dominant effect on the mechanical property results [22–25]. The concentrations of transmutation products produced in these irradiations are not believed to have a significant influence on the hardening resulting from irradiation [22–25]. Additional experiments

Table 2
Summary of Irradiation Temperature, Neutron Fluence, and Calculated DPA values for LCAC, ODS, and TZM Molybdenum [22–25].

Target irradiation temperature[1] (°C)	Actual specimen irradiation temperature[5] (°C)	Irradiation cycles[3]	Neutron fluence ($E > 0.1$ MeV), $\times 10^{24}$ n/m^2/(estimated molybdenum DPA)[2]:capsule ID				
Alloy			LCAC	LCAC	TZM	ODS	LCAC & TZM & ODS
300	270	380	10.5/(0.6):b1	N/A[4]	N/A	N/A	N/A
300	294	388–397	N/A	N/A	N/A	N/A	232/(12.3):f1/f2
600	605	380&381	16.2/(0.9):b2	27.0/(1.4):b5	N/A	N/A	N/A
600	609	388–390	N/A	N/A	72.6/(3.9):n2	72.6/(3.9):n1	N/A
600	560	388–397	N/A	N/A	N/A	N/A	246/(13.1):f4
600	784	388–397	N/A	N/A	N/A	N/A	246/(13.1):f3
968	870	380	N/A	N/A	N/A	22.8/(1.2):k1	N/A
968	870	380–382, 372C	N/A	N/A	N/A	64.4/(3.4):k2	N/A
1000	935	382	18.0/(1.0):b3	N/A	N/A	N/A	N/A
1000	935	380–382	44.6/(2.4):b6	62.7/(3.3):b8	N/A	N/A	N/A
1000	906	388–390	N/A	N/A	73.3/(3.9):n4	N/A	N/A
1000	936	388–397	N/A	N/A	N/A	N/A	247/(13.1):f5/f6
1200	1100	380&381	22.9/(1.2):b4	44.7/(2.4):b7	N/A	N/A	N/A
1200	1100	380–382	61.3/(3.3):b9	N/A	N/A	N/A	N/A

[1]The target irradiation temperature was the calculated tensile specimen temperature objective for the irradiation test. The irradiation temperatures were generally within ±50 °C for irradiations at 300 °C and 600 °C, and 100 °C for irradiations performed at 1000 °C. All irradiations were performed at 85 MW reactor power.
[2]The conversion from neutron fluence to molybdenum dpa for the HFIR spectrum was determined using the code SPECTER [41].
[3]Cycles 380, 381, 382, and 372C were performed from 15 June 2000–1 October 2000 with the MW days and hours of operation as follows: (1) cycle 380 (2230 MW days and 628.8 h), (2) cycle 381 (2123 MW days and 600 h), (3) cycle 382 (1755 MW days and 494.7 h), and (4) cycle 372C (302 MW days and 85.3 h). Cycles 388–397 were performed over a period of 26 July 2002 to 17 November 2003: cycle 388 (2094 MW days and 591.2 h), cycle 389 (2124 MW days and 599.7 h), cycle 390 (2111 MW days and 596.1 h), cycle 391 (2090 MW days and 590.0 h), cycle 392 (2077 MW days and 586.5 h), cycle 393 (2143 MW days and 605.0 h), cycle 394 (2130 MW days and 601.3 h), cycle 395 (2198 MW days and 620.6 h), cycle 396 (2203 MW days and 621.9 h), cycle 397 (2216 MW days and 625.8 h).
[4]N/A indicates that irradiations were not performed at these conditions.
[5]Actual Specimen irradiation temperatures for each capsule are reported [22–25].

will be needed to more clearly separate the contribution of the defects produced by irradiation and the transmutation products on the changes in mechanical properties and irradiation hardening [22–25].

The hardness measurement and annealing methods were the same as used for the lower fluence LCAC specimens in a previous study [25]. Vicker's hardness measurements were determined at room-temperature from a single tensile specimen in each of the non-irradiated, post-irradiated, and post-irradiated + annealed conditions. A Buehler microhardness tester was used in the grip region of room-temperature tensile specimens with a dwell time of 5 s with a 500 or 1000 g load. No significant difference in hardness was determined for measurements taken with a 500 or 1000 g load, but less scatter was generally produced with a 1000 g load. The distance from the specimen edge was always larger than ten (10) diagonals of the indenter to avoid edge effects [56]. The hardness was taken as the average of four to ten measurements. Post-irradiated annealing was performed in a vacuum furnace ($<6 \times 10^{-5}$ MPa) that had molybdenum heating elements and heat shields. The specimens were heated to temperature in 30–45 min. Isochronal anneal hold times were for 1-hour, while the isothermal anneal was performed at 700 °C for cumulative times of 0.5–64 h.

3. Results and discussion: Post-irradiation hardness and isochronal annealing

LCAC, TZM, and ODS are wrought flat products that have microstructures consisting of elongated, pancaked grains aligned in the longitudinal orientation [22–25], see Table 1. LCAC has a low volume fraction of inclusions, while TZM has a higher volume fraction of equiaxed carbide particles. ODS has the highest volume fraction of particles (La-oxides) that can be either aligned in the working direction or dispersed as sub-micron sized particles [49–53].

3.1. Change in hardness after irradiation

A summary of the non-irradiated and post-irradiated hardness values is provided in Table 3 with a plot of hardness versus fluence given in Fig. 1. All hardness measurements were made on the as-electropolished surface of the tensile specimens, which may result in some scatter in values. Direct relationships between irradiated hardness and tensile strength have been reported in the literature for irradiated molybdenum [8,9], but such a correlation cannot be made in this work. However, the relative trends between the hardness and room-temperature tensile data generally were similar [25]. Large increases in hardness and tensile strength were observed for irradiation of ODS, LCAC, and TZM at nominal temperatures of 300 °C (270–384 °C) and 600 °C (560–609 °C), while smaller changes in hardness and tensile strength are observed following irradiation at a nominal temperatures of 900 °C (870–936 °C). Irradiation at 900 °C results in the formation of coarse voids that result in small amounts of hardening for ODS and TZM. These alloys are not subject to recrystallization at that temperature. The reason for the small decrease in hardness for 900 °C irradiated ODS at the lowest dose is not clear, as coarse voids have been observed that produce small increases in tensile strength [24]. Recrystallization of LCAC molybdenum would be expected to occur during long-term exposures at 900 °C, and the increase in grain size would result in a decrease in both strength and hardness [22,25]. Recrystallization of LCAC molybdenum during the 900 °C irradiations would be expected to produce an initial decrease in hardness for lower fluence irradiations followed by small amounts of hardening at higher fluences to result in little net change in hardness relative to non-irradiated stress-relieved material. Comparison of post-irradiated hardness to recrystallized LCAC [25] indicates that a low level of irradiation hardening has occurred. The hardness values for 900 °C irradiated TZM molybdenum tended to be slightly higher than ODS. The fine grain size and increased initial dislocation density for as-worked high-purity molybdenum and as-worked ODS molybdenum resulted in slightly lower irradiation hardening than for LCAC and ODS molybdenum for 300 °C and 600 °C irradiations at low fluences [26]. The closer spacing of pre-existing sinks for as-worked high-purity molybdenum and as-worked ODS molybdenum likely reduces the concentration of hardening barriers, but higher fluence irradiations are needed to determine the longevity of this benefit.

Table 3
Summary of average Vicker's hardness values for LCAC, ODS, and TZM molybdenum sheet in the non-irradiated and post-irradiated condition. All alloys are in the stress-relieved condition.

Alloy	Irradiation temperature (°C)/capsule	Average Vicker's hardness value ± standard deviation (MPa) for a given neutron fluence value, × 10^{24} n/m^2 (E > 0.1 MeV)				
		0	10.5–22.9	27.0–44.7	61.3–73.3	232–247
LCAC	270/b1	257.4 ± 3.6 259.6 ± 5.8 265.6 ± 3.6	401.9 ± 4.4 394.0 ± 3.9	N/A	N/A	N/A
	384/f2	272.5 ± 3.3	N/A	N/A	N/A	531.9 ± 15.5
	605/b2 & b5	257.4 ± 3.6 259.6 ± 5.8 265.6 ± 3.6	324.4 ± 5.4 325.6 ± 5.1 337.4 ± 8.9	379.3 ± 1.5 402.2 ± 8.3	N/A	N/A
	560/f4	272.5 ± 3.3	N/A	N/A	N/A	547.4 ± 19.1
	935/b3, b6, b8	257.4 ± 3.6 259.6 ± 5.8 265.6 ± 3.6	194.8 ± 1.7 206.2 ± 5.4	184.8 ± 4.2 196.2 ± 4.0 204.3 ± 3.9	152.6 ± 4.1 160.6 ± 6.1 169.0 ± 4.0	N/A
	936/f6	272.5 ± 3.3	N/A	N/A	N/A	265.5 ± 7.9
	1100/b4, b7, b9	257.4 ± 3.6 259.6 ± 5.8 265.6 ± 3.6	167.2 ± 3.3	167.4 ± 2.0 170.6 ± 6.2	175.3 ± 4.5 178.9 ± 3.7	N/A
ODS	384/f2	263.9 ± 4.9	N/A	N/A	N/A	521.6 ± 11.1
	609/n1	261.0 ± 3.8	N/A	N/A	439.1 ± 6.0	N/A
	560/f4	263.9 ± 4.9	N/A	N/A	N/A	552.6 ± 13.0
	870/k1, k2	242.5 ± 3.0 252.7 ± 1.6	233.7 ± 4.4 240.5 ± 6.3 241.0 ± 4.2	N/A	264.5 ± 4.5 265.2 ± 6.7	N/A
	936/f6	263.9 ± 4.9	N/A	N/A	N/A	310.8 ± 4.2
TZM	384/f2	301.3 ± 6.4	N/A	N/A	N/A	534.5 ± 3.8
	609/n2	296.5 ± 1.4	N/A	N/A	556.5 ± 14.8 564.3 ± 8.1	N/A
	560/f4	263.9 ± 4.9	N/A	N/A	N/A	610.4 ± 11.4
	906/n4	296.5 ± 1.4	N/A	N/A	342.4 ± 8.3	N/A
	936/f5	263.9 ± 4.9	N/A	N/A	N/A	309.3 ± 14.0

[1]Each value is the average of 4–10 measurements.
[2]Multiple values for each condition represent duplicate measurements made on the same or alternate specimens.
[3]Hardness measurements for capsules b1-b9, k1-k2 were performed at 500 g load, while 1000 g load was used for capsules, n1, n2, n4, and f1-f6.

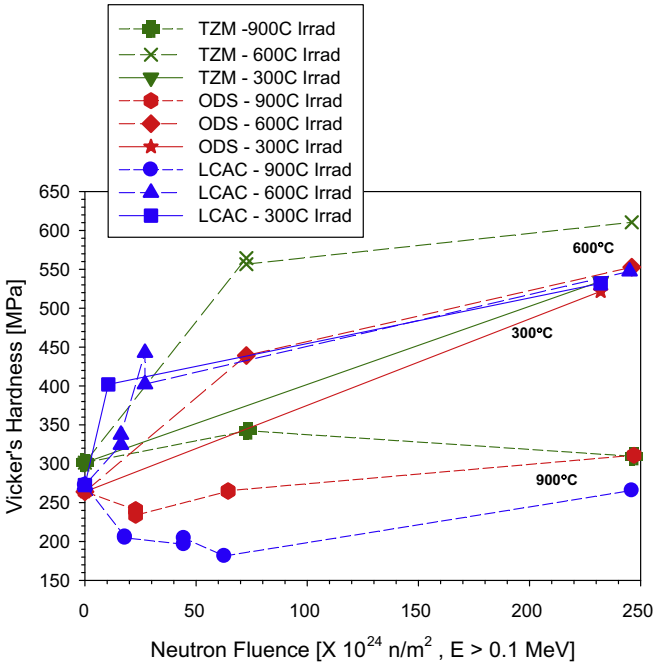

Fig. 1. Hardness values as a function of neutron dose for the irradiation of ODS, LCAC, and TZM molybdenum at 300 °C, 600 °C, and 900 °C. The hardness values are the average of 4–10 measurements, and are listed in Table 3.

It is interesting to note that the high-fluence hardness values for the 600 °C irradiations are slightly higher than those obtained at 300 °C. This trend is stronger in TZM than either LCAC or ODS. This result seems to run contrary to the expectation that greater hardening would be produced by the higher number density of voids and loops expected at 300 °C (nominally 8.3–8.7 × 10^{17} #/cm^3 [6–20]) compared to those present at 600 °C (nominally 1.7–3.0 × 10^{17} #/cm^3) at the highest dose. The larger void size reported in the literature [6–20] for irradiations at 600 °C (5–6 nm) than for 300 °C (~1 nm) creates stronger barriers that likely compensates for the slightly lower void number density to give slightly greater hardening for the 600 °C irradiations. Wirth [59,60] and Hatano and Matsui [61] have recently demonstrated via atomistic calculations that larger voids might be more effective at trapping dislocations than smaller ones. It is possible that the increased void size at higher temperature compensates for the commensurate reduction in the number density. More detailed study will be needed to address this issue.

It also is interesting to note from Fig. 1 that hardening appears to saturate with fluence, suggesting an asymptotic approach to a steady-state microstructure. This interpretation is more conclusive in the case of hardness data than the tensile tests reported previously [22–24]. In tensile tests, once the material has hardened to the point where fracture occurs before yield, it is difficult to determine if any additional increase in yield stress takes place with increasing dose. The data shown here suggest that the fluence at which saturation occurs increases with increasing irradiation temperature.

3.2. Change in hardness after isochronal annealing

Isochronal annealing results for the irradiations of LCAC, ODS, and TZM at nominal temperatures of 300 °C and 600 °C are shown in Figs. 2(a), 3(a) and (b), respectively. The recovery of hardness begins at a temperature between 530 °C and 890 °C (Table 4) depending on the irradiation temperature, neutron fluence, and

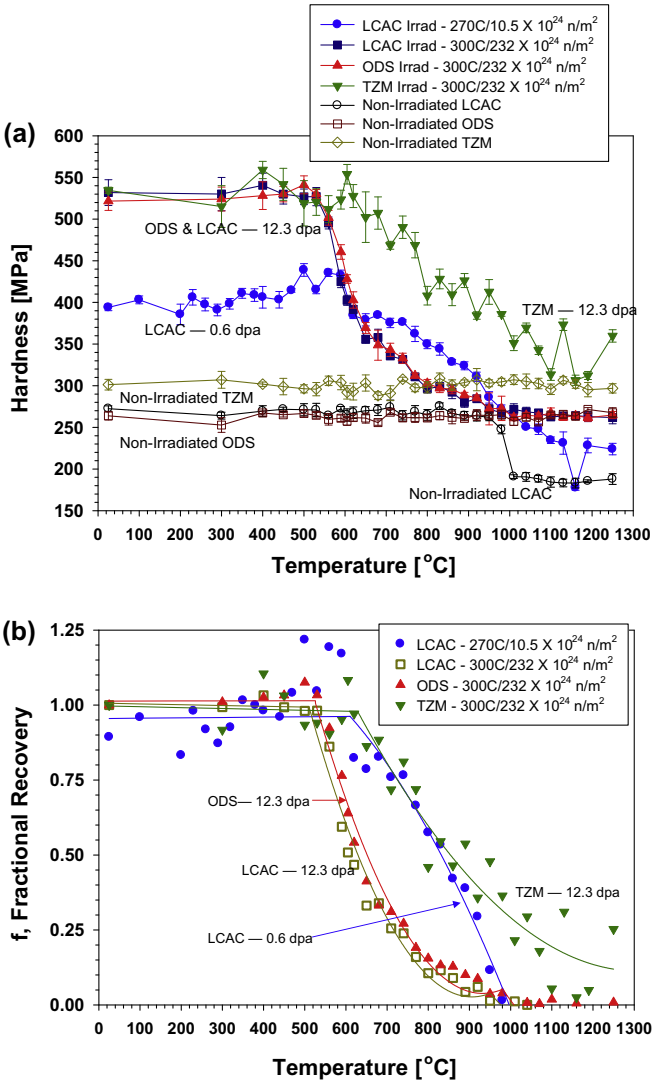

Fig. 2. Plot of isochronal annealing results (1-hour anneals) for ODS, LCAC, and TZM molybdenum irradiated at nominally 300 °C (270–384 °C) to a nominal fluence of 10.5 (LCAC only) and 232 × 10^{24} n/m^2 ($E > 0.1$ MeV) compared to a non-irradiated control: (a) plot of average hardness versus isochronal annealing temperature with the error bars representing one standard deviation, and (b) plot of calculated fractional recovery, f, from Eq. (1) as a function of isochronal annealing temperature. All materials were in the stress-relieved condition. Results for LCAC at the low dose were previously reported [25].

material condition. This is consistent with the Stage V recovery temperature (≈600 °C) in molybdenum [25,28]. The start temperature for recovery exhibited no clear trend with respect to dose for each respective alloy. The temperatures for the onset of recovery were lower, in general, for the irradiations at a nominal temperature of 300 °C compared to materials irradiated at 600 °C. This is consistent with the higher number density of smaller voids and loops observed for 300 °C irradiations [6–20] providing a shorter diffusion distance for void coarsening and a resultant recovery of hardness. The decreases in hardness during the isochronal annealing are expected to result from the coarsening of voids with a decrease in void number density, which has been observed to occur at annealing temperatures (600–1100 °C) that are comparable to or higher than Stage V recovery temperatures, by the solid-state diffusion of vacancies [3,4,7–13,28–35]. Examinations of microstructure showed that annealing of 300 °C irradiated ODS molybdenum to a temperature of 600 °C for about 0.5-hour results in an increase in as-irradiated nominal void and loop diameter from 0.9 to 1.5 nm and 3–3.3 nm, respectively, to 2 nm diameter for voids and 7 nm diameter for loops. The kinetics of point defect diffusion that produces this coarsening are discussed in the following section.

A small amount of Radiation Anneal Hardening (RAH) was previously observed for LCAC irradiated to lower fluences (1–14% increase) [25]. This was suggested to result from either the coarsening of point defect loops and clusters or the diffusion of interstitial impurities to defect clusters to form stronger barriers at annealing temperatures between 300 °C and 800 °C [7,36–39]. In the present work, a slight amount of RAH (1–15% increase in hardness) was also observed for LCAC, ODS, and TZM irradiated at nominal temperatures of 300 °C and 600 °C to a higher fluence (232–246 × 10^{24} n/m^2) when annealed between 400 °C and 600 °C. This behavior is similar to the RAH previously observed for LCAC irradiated to lower fluences [25]. No trend was observed with respect to irradiation temperature or alloy for RAH. The observed RAH is a small fraction of the fractional increase in hardness from irradiation for LCAC, ODS and TZM (77–109% increase) indicating that the strengthening barriers produced by irradiation dominate the mechanical properties and are of most interest [7,25].

The annealing temperature at which full recovery to the non-irradiated hardness levels occurs for 300 °C irradiated LCAC and ODS is 980 °C for the irradiation doses studied (see Fig. 2 and Table 4). Irradiation of LCAC at 300 °C to high fluence produces higher amounts of hardening. The recovery observed for LCAC irradiated at 300 °C to high dose is shown in Fig. 2 to start at a slightly lower temperature and proceed faster than the recovery of the low dose irradiations at isochronous annealing temperatures between 650 °C and 950 °C. Between the temperatures of 650 °C and 1000 °C the hardness of the high dose irradiation sample drops below that of the low dose sample even though the initial values were much higher. However, full recovery was achieved for both high and low dose material at the same isochronous annealing temperature of 980 °C. The faster initial recovery observed for LCAC irradiated at 300 °C to high dose may result from the more developed defect structure consisting of a higher number density of smaller voids and loops [6–20]. The closer spacing of defects results in shorter diffusion distance for void/loop coarsening so that the recovery of hardness can occur more readily. The smaller defect clusters observed at lower irradiation temperature may also store considerably more strain energy. Therefore, the energetic impetus to grow may be increased.

The LCAC and ODS molybdenum irradiated at 300 °C to high dose are shown in Fig. 2(a) to exhibit nearly identical recovery kinetics. Both LCAC and ODS consist of a molybdenum matrix with no real difference in alloying content or impurity content though ODS has a finer grain size and oxide particle size, with pan-caked shaped grains of 2.5–1.2 μm thickness and 46–33 μm length for ODS compared to 5.0–3.9 μm thickness and 172–78 μm length for LCAC [22–25]. The similarity in recovery kinetics for ODS and LCAC irradiated at 300 °C indicates that the recovery is controlled by the diffusion of point defects in the bulk of the grains and the higher fraction of boundary area that results from the finer grain size and oxide particles has no apparent effect on the diffusion of point defects that produce recovery. Recovery of 300 °C irradiated TZM during isochronal annealing starts and finishes at a higher temperature and is much more gradual than observed for LCAC and ODS. TZM molybdenum has a small amount of titanium and zirconium in solid-solution with some (Ti,zr)-rich carbide particles. The presence of titanium and zirconium in solid solution likely serves to trap or slow the diffusion of point defects within the grains to result in slower recovery than observed for LCAC and ODS. The isochronal annealing recovery of dilute Mo–Ti and Mo–zr alloys irradiated at about

150 °C has been reported in the literature to be slower than unalloyed molybdenum [39].

Recovery for 600 °C irradiated LCAC is observed to be completed at 1010 °C, 1070–1130 °C, and 1190 °C annealing temperatures for the neutron fluences of 16.2, 27.0, and 246 × 10^{24} n/m^2, respectively. The temperatures for full recovery of the LCAC irradiated at nominally 300 °C and 600 °C are generally within the range of temperatures reported in literature (1000–1200 °C) for lower dose irradiations at 70–700 °C (see Table 4). Recovery of ODS and TZM irradiated at 600 °C is observed to occur at higher temperatures than LCAC with even higher annealing temperatures required at higher dose (see Table 4). The higher increase in hardness at higher dose results from a higher number density of smaller voids being formed [6–20]. However, higher isochronal annealing temperatures are required for the defect structures produced at higher dose to recover. This is in direct contrast to the dose dependence observed for the 300 °C irradiations where the recovery was faster for the higher dose irradiation. The formation of irradiation-induced defect complexes or phases based on transmutation products at high dose [6–20] for the 600 °C irradiations (but not in the 300 °C tests due to the slower diffusion kinetics) may produce the slower recovery kinetics but more investigations are needed to corroborate this hypothesis.

As observed for the 300 °C irradiations, the recovery kinetics for LCAC and ODS irradiated at 600 °C to high dose appear to be identical. However, the recovery of ODS becomes slower than LCAC at isochronal annealing temperatures greater than 1100 °C and the recovery of ODS is not complete at 1250 °C. ODS is more resistant

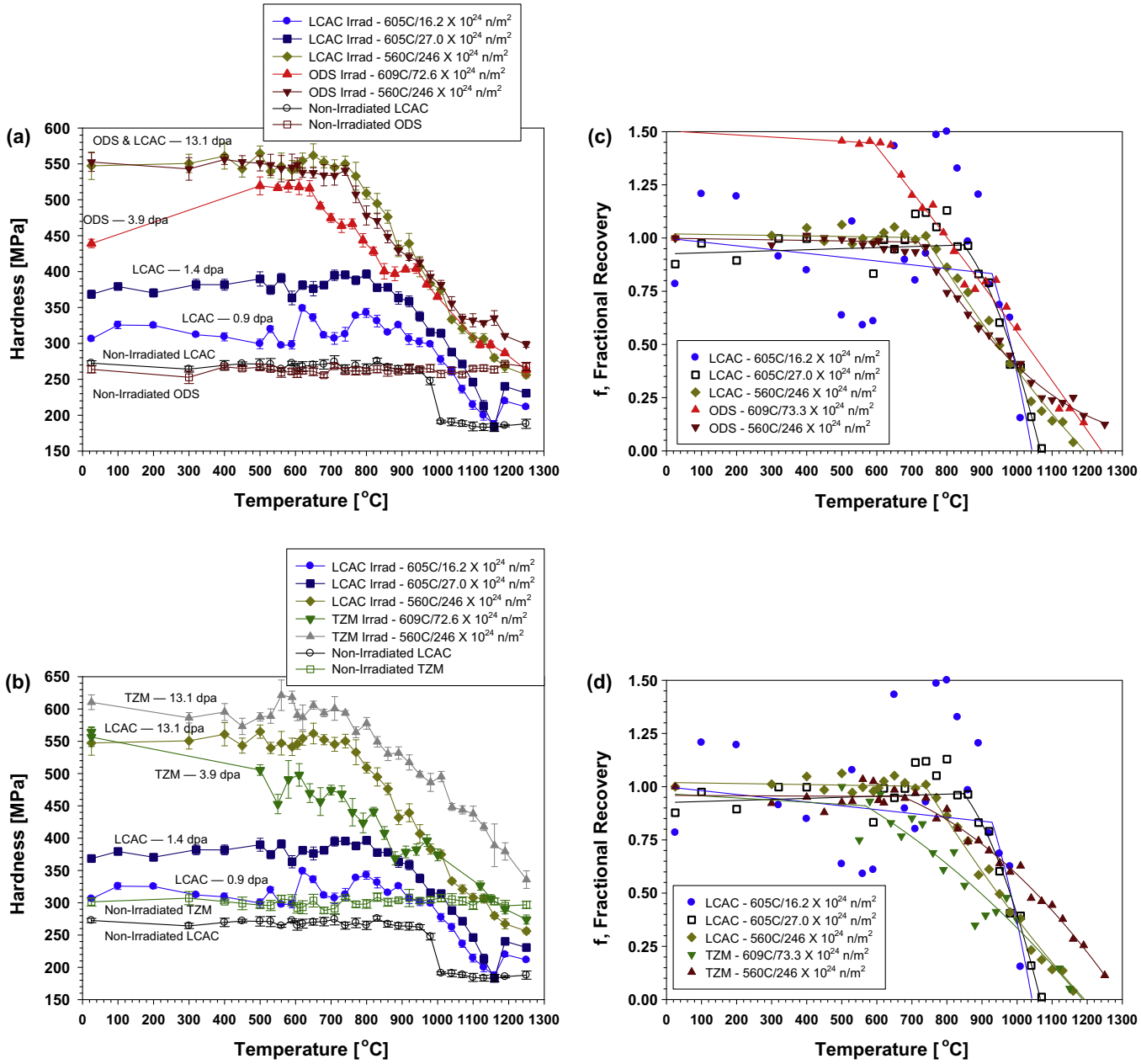

Fig. 3. Plots of post-irradiated hardness values for the isochronal annealing (1-hour anneals) of ODS, LCAC, and TZM molybdenum that were irradiated at nominally 605 °C to a nominal fluence of 16.2 × 10^{24} n/m^2 and 27.0 × 10^{24} n/m^2 (E > 0.1 MeV) for LCAC, 72.6 × 10^{24} n/m^2 for ODS and TZM, and 246 × 10^{24} n/m^2 for all alloys. All materials were in the stress-relieved condition, and results for non-irradiated control are shown: (a) average hardness for LCAC and ODS with error bars for one standard deviation, (b) average hardness for LCAC and TZM with error bars representing one standard deviation, (c) fractional recovery, f (Eq. (1)) for LCAC and ODS, and (d) fractional recovery, f (Eq. (1)) for LCAC and TZM. The results for LCAC irradiated to a dose of 16.2 × 10^{24} n/m^2 and 27.0 × 10^{24} n/m^2 were previously reported [25].

Table 4
Summary of temperatures for the start and finish of recovery determined from 1-hour isochronal anneals using hardness measurements.

Irradiation temperature (°C)	Neutron fluence ($\times 10^{24}$ n/m^2, $E > 0.1$ MeV)	Recovery temperatures (°C)	
		Start of recovery	Complete recovery
LCAC molybdenum			
270	10.5	590	980
384	232	530	980
605	16.2	890	1010
605	27.0	830	1070
560	246	740	1190
935	18.0	RT[2]	RT[2]
935	44.6	RT[2]	RT[2]
935	62.7	RT[2]	RT[2]
1100	22.9	RT[2]	RT[2]
1100	44.7	RT[2]	RT[2]
1100	61.3	RT[2]	RT[2]
ODS molybdenum			
384	232	530	980
609	72.6	670	1250
560	246	740	>1250
870	22.9	RT[2]	RT[2]
870	64.4	RT[2]	RT[2]
936	247	RT[2]	RT[2]
TZM molybdenum			
384	232	620	1160
609	73.3	580	1150
560	246	680	>1250
906	73.3	RT[2]	RT[2]
Literature data[4]			
455 – [3]	250	N/A	1050
70 – [8,9]	1.1	N/A	1200
430 – [11]	~100[5]	N/A	1450
70 – [28]	1.4	N/A	1000
40 – [29]	0.4[5]	N/A	800
40 – [30]	0.062[5]	N/A	1000
465 – [6]	140	N/A	1050
450 – [31]	0.7[5]	N/A	1050
470 – [32]	40[5]	N/A	1100
150 – [39]	0.09[5]	N/A	1000

[1]All materials are in the stress-relieved condition.
[2]No recovery was observed for materials irradiated at nominally 900 °C (870 °C-936 °C).
[3]The low dose results for LCAC were previously reported [25].
[4]The reference number is indicated for irradiation temperature.
[5]The neutron fluence for these earlier studies is in terms of $E > 1$ MeV. A rough estimate for fluence in terms of $E > 0.1$ MeV can be obtained by multiplying the fluence ($E > 1$ MeV) times a factor of 2.
[6]N/A means this property was not measured.

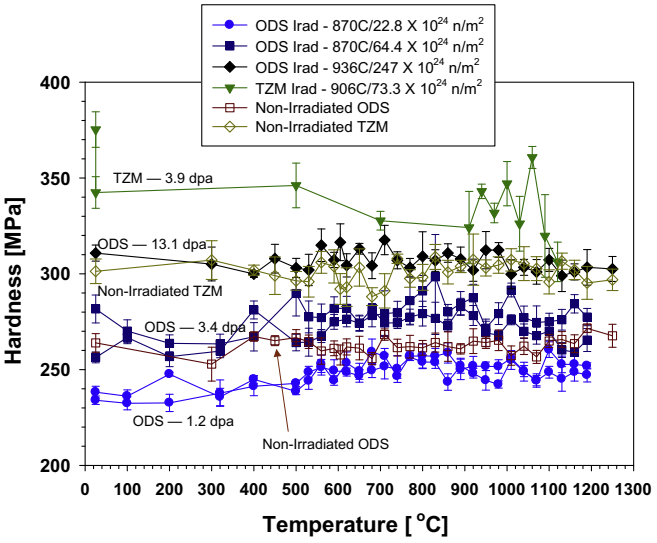

Fig. 4. Plot of Vicker's hardness versus isochronal annealing temperature (1-hour anneals) for ODS and TZM molybdenum irradiated at nominally 900 °C (870–936 °C) to a nominal fluence of 22.8, 64.4, and 247 $\times 10^{24}$ n/m^2 ($E > 0.1$ MeV) for ODS and 73.3 $\times 10^{24}$ n/m^2 for TZM. The average hardness values are plotted with error bars that represent one standard deviation. All materials were in the stress-relieved condition. Results for non-irradiated ODS and TZM molybdenum are also shown.

to recrystallization and the finer grain size and particle size/volume fraction for ODS may result in a closer spacing of sinks for vacancies and closer spacing of void denuded zones. Thus, the irradiation produced vacancy concentration may be reduced and void coarsening that produces recovery is slowed at higher isochronal annealing temperatures where the vacancy mobility is higher. The finer grain size and spacing of particles for ODS results in improved extrinsic fracture resistance and is expected to result in a slightly higher fraction of void denuded zones. It also results in a lower DBTT (room-temperature) for 600 °C irradiated ODS in comparison to TZM or LCAC (300–700 °C) [23,24]. TZM irradiated at 600 °C starts recovery at a higher temperature and isochronal recovery for TZM is slower than observed for LCAC and ODS. As seen in the 300 °C experiment, this may be explained by the presence of Ti + zr solutes in TZM that trap or slow the movement of vacancies that is needed for recovery [39].

Little irradiation hardening and no resolvable change in hardness was observed in Fig. 4 for the isochronal annealing (up to 1250 °C) of TZM and ODS that had been irradiated at 900 °C. This is similar to the result previously observed for LCAC irradiated at 935 °C and 1100 °C to a lower dose [25]. Post-irradiated TEM examinations of microstructure reported in the literature [6–20] have indicated that a low number density of coarse voids would be expected for irradiations of LCAC, ODS, and TZM at nominally 900 °C that result in little irradiation hardening. The coarse voids formed by the 900 °C irradiations are widely spaced and the fact that no change in hardness during the annealing runs is observed indicates that the size and number density of voids probably has not changed. These results indicate that the coarse void structure that is formed by the 900 °C irradiation of LCAC, ODS, and TZM is resistant to coarsening at temperatures as high as 1250 °C for 1-hour.

4. Results and discussion: Recovery kinetics for 300 °C and 600 °C irradiations

Isothermal annealing of LCAC, ODS, and TZM irradiated at nominally 300 °C and 600 °C was performed at 700 °C to determine the kinetics for recovery using the Meechan–Brinkman method of analysis [45–47]. The same approach was used previously for LCAC irradiated to lower dose [25]. The fraction of recovery (f) for post-irradiated isochronal annealing, shown in Figs. 2(b), 3(c) and (d) for the 300 °C and 600 °C irradiations, respectively, was defined as

$$f = (H_a - H_{NI})/(H_{AR} - H_{NI}), \quad (1)$$

where H_a is the hardness at the isochronal annealing temperature, H_{AR} is the as-irradiated hardness, and H_{NI} is the non-irradiated hardness [25]. The general form for the recovery rate is given as follows [46]

$$-df/dt = K(T)F(f), \quad (2)$$

where $F(f)$ is the Arrhenius function for a single recovery process defined by the rate constant

$$K(T) = v_o \exp(-E_a/KT), \quad (3)$$

E_a is the activation energy of the recovery process, v_o is the frequency factor, and k is Boltzmann's constant. Substitution of

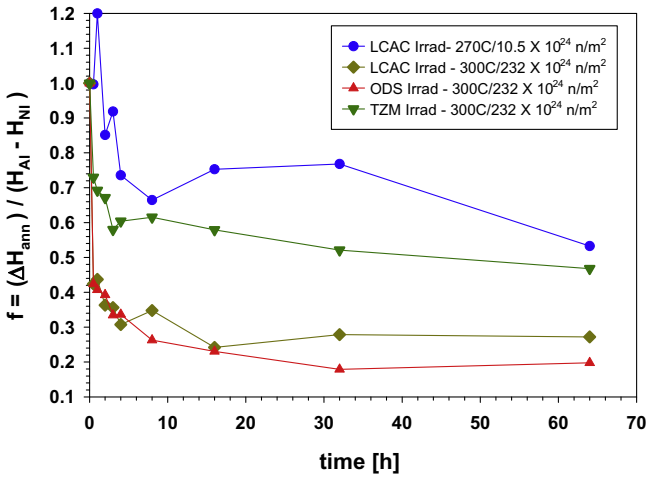

Fig. 5. Plot of fraction of recovery (Eq. (5)) versus annealing time for the 700 °C isothermal annealing for stress-relieved ODS, LCAC, and TZM molybdenum irradiated at nominally 300 °C to a fluence of 10.5×10^{24} n/m^2 (0.6 dpa) for LCAC only [25] and 232×10^{24} (12.3 dpa) for ODS, LCAC, and TZM.

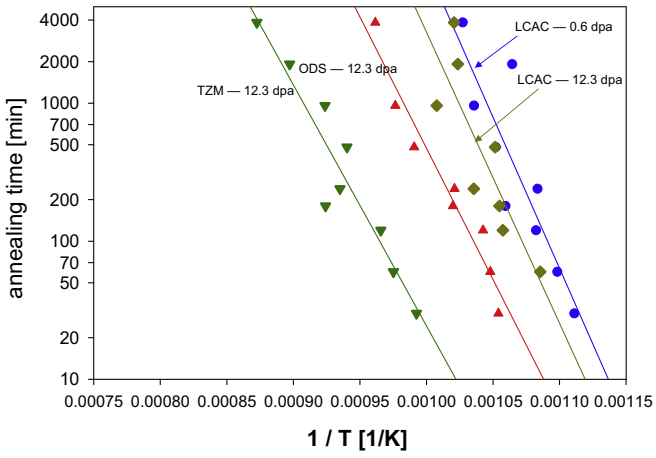

Fig. 6. Semi-log plot of isothermal time interval versus inverse isochronal annealing temperature used to determine activation energy using the Meechan–Brinkman method for stress-relieved ODS, LCAC, and TZM molybdenum irradiated at nominally 300 °C to a fluence of 10.5×10^{24} n/m^2 (0.6 dpa) for LCAC only [25] and 232×10^{24} (12.3 dpa) for ODS, LCAC, and TZM.

Eq. (3) in Eq. (2) with integration gives the equation used in the Meechan–Brinkman analysis,

$$(1/v_o)g(f) = (1/v_o)\int \mathrm{d}f/F(f) = t\ \exp(-E_a/KT), \tag{4}$$

The fractional recovery from isothermal annealing was determined using the difference in hardness between the irradiated specimen and average for the non-irradiated control, ΔH

$$f = \Delta H/(H_{AR} - H_{NI}). \tag{5}$$

The plots of fractional recovery for the isochronal anneals shown in Figs. 2(b), 3(c) and (d) can be used to define the start of recovery, finish of recovery, and RAH that were discussed in the previous section. A second order fit for fractional recovery versus isochronal annealing temperature was used to describe the recovery of hardness [25]. Recovery was observed during the isothermal annealing of 300 °C and 600 °C irradiated LCAC, ODS, and TZM, shown in Figs. 5 and 7, respectively. The recovery was more complete and faster for 300 °C irradiated LCAC, ODS, and TZM than for the 600 °C irradiations during the isothermal annealing. The higher number density of defects (voids/loops) and smaller defect size from the 300 °C irradiations provides a smaller diffusion distance that results in faster and more significant recovery.

For the 300 °C irradiations, the recovery was faster and larger recovery values were observed for the higher dose irradiations compared to the lower dose results for LCAC. The formation of a slightly smaller void/loop size and a higher number density at higher dose may shorten the spacing between defects resulting in faster recovery. No RAH was observed during the isothermal annealing of LCAC, ODS, and TZM irradiated to high dose. This may be a result of maturation of the irradiated microstructure where the point defect clusters or interstitial solutes that could possibly lead to RAH are moved to voids or loops during irradiation. Fig. 5 shows that the recovery behaviors of 300 °C irradiated LCAC and ODS are similar during the isothermal anneal while the recovery for TZM was much slower. The same trend was observed for isochronal annealing of 300 °C irradiated materials. TZM has a small fraction of titanium and zirconium solute atoms and carbide precipitates rich in titanium and carbon that can slow or trap vacancies so that the recovery of hardness is slower.

In contrast to the high dose samples for the 600 °C irradiations, RAH is observed for both LCAC irradiated at 605 °C to low dose and then subsequently annealed for 0.5 h to 3 h and TZM irradiated at

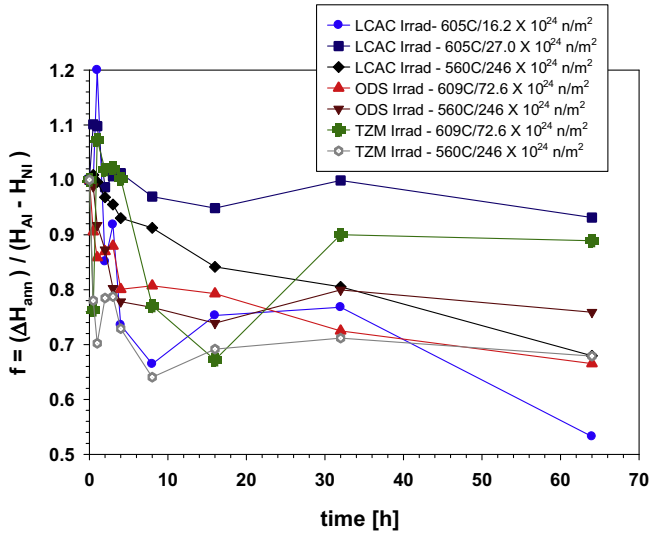

Fig. 7. Plot of fraction of recovery (Eq. (5)) versus annealing time for the 700 °C isothermal annealing for stress-relieved ODS, LCAC, and TZM molybdenum that were irradiated at nominally 600 °C to a fluence of 16.2 and 27.0×10^{24} n/m^2 (0.9 and 1.4 dpa) for LCAC only [25] and 246×10^{24} (13.1 dpa) for ODS, LCAC, and TZM.

600 °C to a fluence of 72.6×10^{24} n/m^2 and then annealed for 32 and 64 h. RAH likely results from either the coarsening of point defects to form larger defects or the movement of interstitial or other solute atoms to voids that result in the formation of stronger barriers to dislocation motion, but examinations of microstructure are required to confirm the source of RAH. RAH of irradiated molybdenum has been reported to occur at annealing temperatures between 300 °C and 800 °C [7,36–39]. No RAH was observed for ODS irradiated at 600 °C to a lower fluence (72.6×10^{24} n/m^2).

Irradiation at 600 °C to high fluence did not significantly change the amount or rate of recovery for LCAC and ODS during the isothermal anneal compared to that observed for lower fluence irradiations. Irradiation at 600 °C to higher fluence results in the formation of a higher number density of smaller voids and a shorter diffusion distance for recovery. The recovery of 600 °C irradiated TZM during the isothermal annealing was very different than LCAC and ODS.

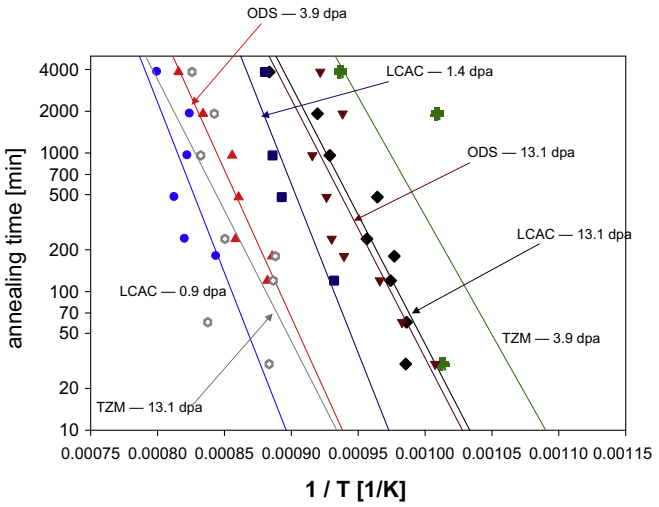

Fig. 8. Semi-log plot of isothermal time interval versus inverse isochronal annealing temperature used to determine activation energy using the Meechan-Brinkman method for stress-relieved ODS, LCAC, and TZM molybdenum that were irradiated at nominally 600 °C to a fluence of 16.2 and 27.0 × 10^{24} n/m^2 (0.9 and 1.4 dpa) for LCAC only [25] and 246 × 10^{24} (13.1 dpa) for ODS, LCAC, and TZM.

Figs. 6 and 8 show the Arrhenius plots of isothermal annealing times versus the inverse isochronal annealing temperature at which the fraction of recovery is equivalent for the 300 °C and 600 °C irradiations. This is used to determine activation energies for annealing recovery using the Meechan–Brinkman method [25,45–47]. Values where RAH was observed ($f > 1$) were not plotted. Although relatively large scatter in hardness values results in poor fits for some of the Arrhenius plots shown in Figs. 6 and 8, the activation energies provide a relative measure of the kinetic process for recovery. The activation energies for LCAC and ODS irradiated at 300 °C and 600 °C to both high and low dose are shown in Table 5 to be within the range of literature values for self-diffusion in molybdenum. The similarity in activation energy to the value for self-diffusion for 300 °C and 600 °C irradiated LCAC and ODS molybdenum indicates that the recovery process is probably controlled by the solid-state diffusion of vacancies to increase the size of dislocation loops and/or voids and reduce the number density of these defects. The isochronal annealing recovery, isothermal annealing recovery, and activation energy values for LCAC and ODS irradiated at both 300 °C and 600 °C are observed to be similar, which indicates that the recovery process is the same. Although ODS has a finer grain size and fine particle distribution, these differences in structure do not appear to change the kinetics for the vacancy movement that produces recovery. Although the activation energy values for LCAC irradiated at 605 °C to a lower fluence (16.2–27.0 × 10^{24} n/m^2) were slightly higher than the values for molybdenum self-diffusion, lower values that are comparable to those for molybdenum self-diffusion are observed for LCAC irradiated at 600 °C to a higher fluence (246 × 10^{24} n/m^2). Irradiation of LCAC at 600 °C to higher dose results in additional evolution of the microstructure which may alter the recovery kinetics and therefore the activation energy. Alternatively, there may not have been enough data for the lower dose 600 °C irradiations of LCAC to determine the activation energy with a high degree of accuracy. The activation energy values in Table 5 are observed to decrease slightly with higher dose and lower irradiation temperatures. This suggests that the higher number density of defects produced under these conditions may result in a higher concentration of stored energy in these defects which could act as a driving force for accelerated recovery.

The recovery rates for TZM during isochronal and isothermal annealing were slower than observed for LCAC and ODS. The activation energy values for TZM were slightly lower than LCAC and ODS, and were similar to values reported in literature for vacancy mobility in molybdenum (3.3–3.5 eV) [7,40]. The slower recovery rate during isochronal and isothermal annealing for TZM indicates that the presence of titanium and zirconium solutes in TZM have a slowing or trapping effect on the mobility of point defects [39]. The only exception is that TZM irradiated at 600 °C to high dose has an activation energy that is within the range of values for the high dose 600 °C irradiations of LCAC and ODS.

Table 5
Summary of activation energy determined from the 700 °C isothermal anneal using the Meechan–Brinkman analysis for ODS, LCAC, and TZM irradiated at nominally 300 °C and 600 °C compared with literature data.

Irradiation temperature (°C)	Neutron fluence (× 10^{24} n/m^2, $E > 0.1$ MeV)	Isothermal annealing temperature (°C)	Activation energy ± standard deviation (eV)
LCAC molybdenum			
270	10.5	700	4.35 ± 0.28
384	232		4.19 ± 0.43
605	16.2		4.88 ± 0.77
605	27.0		4.83 ± 0.62
560	246		3.70 ± 0.36
ODS molybdenum			
384	232	700	3.77 ± 0.38
609	72.6		4.22 ± 0.37
560	246		3.70 ± 0.36
TZM molybdenum			
384	232	700	3.47 ± 0.36
609	72.6		3.41 ± 0.63
560	246		3.75 ± 0.39
Literature data[1]			
N/A – [7]	N/A[2]	805–897	Stage A – 1.95 Stage B – 3.30
70 – [40]	0.98[3]	800	3.5
70 – [41,42]	0.11-15.0[3]	500–700	1.70 ± 0.15
600 – [34]	11	947–1097	2.0
40 – [29]	0.4[3]	134–167	1.20
Molybdenum self-diffusion[1]			
[7]	N/A	N/A	4.30
[57]	N/A	N/A	4.0
[58]	N/A	N/A	4.0

Complete recovery to non-irradiated values was not observed during isothermal annealing for all specimens.
[1]The reference number is indicated for irradiation temperature, and self-diffusion data.
[2]N/A means this information is not available.
[3]The neutron fluence for these earlier studies is in terms of $E > 1$ MeV. A rough estimate for fluence in terms of $E > 0.1$ MeV can be obtained by multiplying the fluence ($E > 1$ MeV) times a factor of 2.

5. Summary and conclusions

The post-irradiation changes in hardness for ODS, LCAC, and TZM molybdenum were generally similar to the trends previously observed in ultimate tensile strength [21–25]. However, the increases in hardness were the highest for the 600 °C irradiations for each of the alloys, while the ultimate tensile strength values for the 300 °C and 600 °C irradiations were generally comparable because brittle fracture occurred before the samples could yield. Small increases in hardness were generally observed at fluences between 10.5–247 × 10^{24} n/m^2, while saturation of the increase in tensile strength was generally observed at fluences between 10.5 and 61.3 × 10^{24} n/m^2 due to the onset of brittle fracture. The more compressive stress-state for hardness testing allows a better assessment of the effects of irradiation on plastic flow behavior for these embrittled materials as fracture was not produced.

Recovery of hardness for 300 °C and 600 °C irradiated LCAC, ODS, and TZM during isochronal annealing begins at 530 °C and

890 °C, respectively. This is consistent with Stage V recovery in molybdenum (≈600 °C) where vacancy diffusion is active. Full recovery of hardening for LCAC irradiated at 300 °C and 600 °C occurs at isochronal annealing temperatures of 980 °C and 1070–1190 °C, respectively, consistent with literature data (1000–1200 °C).

The recovery behavior of 300 °C and 600 °C irradiated LCAC and ODS are identical with the exception of the slower recovery observed for 600 °C irradiated ODS at temperatures greater than 1100 °C. The activation energy values for the post-irradiation annealing recovery of LCAC and ODS irradiated at 300 °C and 600 °C were shown to be (3.70–4.88 eV ± 0.28–0.77 eV) comparable to values reported for molybdenum self-diffusion (4.0-4.3 eV). Although ODS had a significantly finer grain size and fine distribution of oxide particles, both LCAC and ODS exhibited similar recovery kinetics during isochronal annealing and isothermal annealing at 700 °C. The two materials also exhibited comparable activation energies for recovery. This indicates that the post-irradiation annealing recovery was most likely controlled by vacancy diffusion within the grains and that the grain size and particle size of ODS was not fine enough to affect vacancy diffusion.

TZM exhibited slower recovery than ODS and LCAC during isochronal annealing and isothermal annealing at 700 °C. This indicates that the titanium and zirconium solute atoms have a trapping effect on vacancy mobility [39]. However, the activation energy values are close enough to the reported values for molybdenum self-diffusion to conclude that recovery of TZM is also controlled by the solid-state diffusion of vacancies.

Acknowledgments

This work was supported by USDOE. The authors are grateful for the review and comments provided by J.E. Hack. The assistance of R.F. Luther and A.J Mueller in providing some of the LCAC and ODS molybdenum specimens used in this work is much appreciated. Thanks also to the following ORNL personnel for their contributions in completing irradiations and testing (A.L. Qualls, A.W. Williams, and J.L. Bailey). Irradiations were carried out in the High Flux Isotope Reactor, a Department of Energy Office of Science User Facility.

References

[1] J.B. Lambert, J.J. Rausch, Non-Ferrous Alloys and Special-Purpose Materials, Materials Handbook, vol. 2, ASM International, Materials Park, OH, 1992, pp. 557–582.
[2] S.J. Zinkle, N.M. Ghoniem, Fusion Eng. Des. 51&52 (2000) 55.
[3] F.W. Wiffen, in: R.J. Arsenault (Ed.), Proceedings of the 1973 International Conference on Defects and Defect Clusters in B.C.C. Metals and Their Alloys, Nucl. Metall.18 (1973) p. 176.
[4] B.L. Cox, F.W. Wiffen, J. Nucl. Mater. 85&86 (1979) 901.
[5] R.E. Gold, D.L. Harrod, J. Nucl. Mater. 85&86 (1979) 805.
[6] T.H. Webster, B.L. Eyre, E.A. Terry, in: Proceedings of the Irradiation Embrittlement and Creep in Fuel Cladding and Core Components, November 9–10 1972, British Nuclear Energy Society, London.
[7] J. Moteff, Radiat. Eff. 37 (1965) 727.
[8] K. Furuya, J. Moteff, Metall. Trans. 12A (1981) 1303.
[9] K. Furuya, J. Moteff, J. Nucl. Mater. 99 (1981) 306.
[10] F. Lee, J. Matolich, J. Moteff, Nucl. Technol. 39 (1978) 207.
[11] V.K. Sikka, J. Moteff, Nucl. Technol. 22 (1974) 52.
[12] V.K. Sikka, J. Moteff, J. Nucl. Mater. 54 (1974) 325.
[13] J. Moteff, D.J. Michel, V.K. Sikka, in: R.J. Arsenault (Ed.), Proceedings of the 1973 International Conference on Defects and Defect Clusters in B.C.C. Metals and Their Alloys, Nucl. Metall. 18 (1973) p. 198.
[14] B.N. Singh et al., J. Nucl. Mater. 212–215 (1994) 1292.
[15] B.N. Singh et al., J. Nucl. Mater. 223 (1995) 95.
[16] D.S. Gelles et al., J. Nucl. Mater. 103&104 (1981) 1141.
[17] K. Abe et al., Mater. Trans. JIM 34 (11) (1993) 1137.
[18] UWMAK-III, A Noncircular Tokamak Power Reactor Design, R.W. Conn and G.L. Kulcinski, Fusion Technology Program-Nuclear Engineering Department, University of Wisconsin, Madison, WI, July, 1976.
[19] J. Bentley, F.W. Wiffen, in: Proceedings of the Second Topical Meeting on the Technology of Controlled Nuclear Fusion, Richland, WA, CONF-760935-P1, vol. I, 1973, pp. 209–218.
[20] F.A. Garner, J.F. Stubbins, J. Nucl. Mater. 212–215 (1994) 1298.
[21] A. Hasegawa et al., J. Nucl. Mater. 233–237 (1996) 565.
[22] B.V. Cockeram, J.L. Hollenbeck, L.L. Snead, J. Nucl. Mater. 324 (2004) 77.
[23] B.V. Cockeram, R.W. Smith, L.L. Snead, J. Nucl. Mater. 346 (2005) 145.
[24] B.V. Cockeram, R.W. Smith, L.L. Snead, J. Nucl. Mater. 346 (2005) 165.
[25] B.V. Cockeram, J.L. Hollenbeck, L.L. Snead, J. Nucl. Mater. 336 (2004) 299.
[26] B.V. Cockeram, R.W. Smith, K.J. Leonard, T.S. Byun, L.L. Snead, J. Nucl. Mater. 382 (2008) 1.
[27] R.S. Averback, T. Diaz de la Rubia, Solid State Phys. 51 (1998) 281.
[28] J. Moteff, R.C. Rau, F.D. Kingsbury, in: Proceedings of the Radiation Damage in Reactor Materials, vol. II, IAEA, Vienna, Austria, 1969, p. 269.
[29] H.E. Kissinger, J.L. Brimhall, Scr. Metal. 13 (1979) 327.
[30] G.L. Kulcinski, Phys. Rev. 279 (1969) 676.
[31] S.V. Naidu, A. Sen Gupta, R. Roy, P. Sen, Phys. Lett. A 101 (1984) 512.
[32] B.N. Bykov, M.I. Zakharowa, L.G. Kostromin, V.I. Shcherbak, Phys. Met. Metall. 37 (1974) 34.
[33] J.H. Evans, Philos. Mag. 28 (1973) 1405.
[34] N. Igata et al., J. Nucl. Mater. 103&104 (1981) 1175.
[35] S.A. Fabritsiev et al., J. Nucl. Mater. 233–237 (1996) 526.
[36] D.F. Hasson, R.J. Arsenault, Phys. Status Solidi A 22 (1974) 39.
[37] M. Tanaka, K. Fukaya, K. Shiraishi, Trans. Jpn. Inst. Met. 20 (1979) 697.
[38] N. Igata, K. Miyahara, K. Hakomori, K. Shibata, Rad. Eff. 45 (1980) 247.
[39] S. Morozumi et al., J. Nucl. Mater. 108&109 (1982) 417.
[40] L.K. Keys, J. Moteff, J. Appl. Phys. 40 (1969) 3866.
[41] L.K. Keys, J.P. Smith, J. Moteff, Phy. Rev. Lett. 22 (1969) 57.
[42] L.K. Keys, J. Moteff, J. Appl. Phys. 41 (1970) 2618.
[43] R.C. Rau, J. Moteff, R.L. Ladd, J. Nucl. Mater. 40 (1971) 233.
[44] F. Lee, J. Matolich, J. Moteff, Rad. Eff. 60 (1982) 53.
[45] C.J. Meechan, J.A. Brinkman, Phys. Rev. 103 (1956) 1193.
[46] D.J. Harvey, M.S. Wechsler, in: Proceedings of the Eleventh Conference on Effects of Radiation on Materials, 1982, Scottsdale, AZ, ASTM, Philadelphia, PA, 1982, p. 505.
[47] D. Pachur, Nucl. Technol. 59 (1982) 463.
[48] Standard Specification for Molybdenum and Molybdenum Alloy Plate, Sheet, Strip, and Foil, ASTM B386-95, American Society for Testing and Materials, Philadelphia, PA, 1997.
[49] A.J. Mueller, J.A. Shields, R.W. Buckman Jr., in: G.Kneringer, P. Rodhammer, H. Wildner (Eds.), Proceedings of the Fifteenth International Plansee Seminar, vol. 1, Plansee Holding AG, Reutte, Austria, 2001, pp. 485–497.
[50] R.Bianco, R.W. Buckman Jr., in: Evaluation of Oxide Dispersion Strengthened (ODS) Molybdenum Alloys, 1995 Spring ASM/TMS Symposium on High Temperature Materials, May 19, 1995, GE CR&D Center, Schenectady, NY (Available as WAPD-T-3073, DOE/OSTI, Oak Ridge, TN, 1995).
[51] R. Bianco, R.W. Buckman, Jr., in: A. Crowson, E.S. Chen, J.A. Shields, P.R. Subramanian (Eds.), Molybdenum and Molybdenum Alloys, The Minerals, Metals & Materials Society, Warrendale, PA, 1998, pp. 125–142.
[52] B.V. Cockeram, Met. Trans. 36A (2005) 1777.
[53] B.V. Cockeram, Mater. Sci. Eng. 418A (2006) 120.
[54] L.R. Greenwood, R.K. Smither, Specter: Neutron Damage Calculations for Materials Irradiations, ANL/FPP/TM-197, Argonne National Laboratory, January, 1985.
[55] L.R. Greenwood, F.A. Garner, J. Nucl. Mater. 212–215 (1994) 635.
[56] L.E. Samuels, T.O. Mulhearn, J. Mech. Phys. Solids 5 (1957) 125.
[57] J.L. Brimhall et al., J. Nucl. Mater. 48 (1973) 339.
[58] J. Askill, D.H. Tomlin, Philos. Mag. 8 (1963) 997.
[59] A. Arsenlist, B.D. Wirth, M. Rhee, Philos. Mag. A 84 (2004) 3617.
[60] P. Jing, T. Khraishi, J.A. Young, B.D. Wirth, Philos. Mag. A 85 (2005) 757.
[61] T. Hatano, H. Matsui, Phys. Rev. B 72 (2005) 94.